Applied Catalysis B: Environmental 91 (2009) 507–515

Contents lists available at ScienceDirect

Applied Catalysis B: Environmental

journal homepage: www.elsevier.com/locate/apcatb

Enhancement effect of Ag for Pd/C towards the ethanol electro-oxidation in alkaline media

Son Truong Nguyen [a], Hiu Mung Law [a], Hoa Tien Nguyen [a], Noel Kristian [a], Shuangyin Wang [a], Siew Hwa Chan [b], Xin Wang [a,*]

[a] School of Chemical and Biomedical Engineering, Nanyang Technological University, Singapore, 639798, Singapore
[b] School of Mechanical and Aerospace Engineering, Nanyang Technological University, Singapore, 639798, Singapore

ARTICLE INFO

Article history:
Received 30 March 2009
Received in revised form 10 June 2009
Accepted 19 June 2009
Available online 25 June 2009

Keywords:
Ethanol oxidation
Pd–Ag
Palladium
Silver
Alkaline
Direct ethanol fuel cell

ABSTRACT

Carbon supported Pd–Ag/C catalyst was prepared using co-reduction method. Physicochemical characterization results revealed that alloy nanoparticles with face-centered cubic structure were successfully formed. The electrochemical studies for ethanol oxidation in alkaline media were performed with cyclic voltammetry, linear sweep voltammetry and chronoamperometry methods. The results showed that Pd–Ag/C exhibited an excellent activity, enhanced CO tolerance and better stability than Pt/C and Pd/C, making it a promising anodic catalyst for alkaline direct ethanol fuel cell.

1. Introduction

In recent years, energy demand has been more and more increasing due to the development of industries. Direct alcohol fuel cell (DAFC), as a clean energy conversion device, has attracted a great deal of attention due to its high efficiency, high energy density and low or zero emissions [1–4]. Especially, DAFC is very promising for portable applications. Many studies have been done for direct methanol fuel cell (DMFC) [5–9]. However, methanol is widely known as a toxic and harmful chemical [10–12]. In contrast, ethanol has no toxicity compared to methanol and can be produced in large quantity from fermentation process [11,13]. Moreover, ethanol possesses a higher theoretical energy density (8.01 kWh kg^{-1}) than methanol (6.09 kWh kg^{-1}) and is easy to store and handle [13–15]. Therefore, direct ethanol fuel cell (DEFC) attracts more and more attention recent years [15].

Up to date, most of research on DAFC has been done in acidic media with Pt-based electrocatalysts for the electro-oxidation of alcohols. This largely contributes to the high cost of fuel cells [16–19]. In alkaline media, corrosion is less important and kinetics of alcohol oxidation process is significantly improved [20,21]. Therefore, Pt-free catalysts may be used in alkaline DAFC. This advantage will increase the commercialization probability of DAFC.

Recently, Pd has been found as a good catalyst for the oxidation of ethanol in alkaline solutions and its abundance is at least fifty times more than that of Pt on earth [22,23]. However, the activity of Pd for ethanol oxidation in alkaline media needs to be enhanced. There have been some efforts to improve the performance of Pd, such as those by Shen et al., Zhu et al. and Singh et al., by combining Pd with other metals, metal oxides or metal carbides and some enhancements have been achieved [21,24–27]. In this paper, it is aimed to tune the reactivity of Pd by modifying it with cheaper metals, based on d-band theory. According to d-band theory of Nørskov and co-workers [28–36], the trend of reactivity will follow the trend in d-band center values of overlayer and impurity atoms. When metals with small lattice constants are overlayed or alloyed on metals with larger lattice constants, the d-band center shifts up and vice versa, which subsequently affects the reaction rate. If the d-band center is shifted up, the adsorption ability of the adsorbate onto the metals will be stronger and this may help to improve the electro-oxidation of ethanol on the surface of the metals.

Ag is a metal which is much cheaper and more abundant than Pt. According to Hammer and Nørskov's calculation [29], d-band center of Pd with a lattice value of 3.89 Å will be shifted up when combining with Ag (a = 4.09 Å) [37]. Therefore, Ag was chosen to be alloyed with Pd in this research. Here, we report for the first time the enhanced activity of Pd–Ag/C for the ethanol oxidation in alkaline media compared with Ag/C, Pt/C and Pd/C.

* Corresponding author. Tel.: +65 6316 8866; fax: +65 6794 7553.
E-mail address: WangXin@ntu.edu.sg (X. Wang).

0926-3373/$ – see front matter © 2009 Elsevier B.V. All rights reserved.
doi:10.1016/j.apcatb.2009.06.021

2. Experimental

Chemicals used in this work were deionized water, sodium citrate ($Na_3C_6H_5O_7$) (Sigma–Aldrich), $H_2PtCl_6{\cdot}6H_2O$ (Sigma–Aldrich), $Pd(NO_3)_2{\cdot}xH_2O$ (Sigma–Aldrich), $AgNO_3$ (Sigma–Aldrich), $NaBH_4$ (Sigma–Aldrich), C_2H_5OH (Fluka), Nafion solution (5% in isopropanol and water), and carbon black (Vulcan XC-72, Gashub). All the chemicals were used as received without further purifications.

2.1. Catalyst synthesis

To synthesize electrocatalysts, 100 ml aqueous solution of $Na_3C_6H_5O_7$ and various metal precursors were prepared. Then appropriate amount of 0.01 M $NaBH_4$ (freshly prepared) was added slowly into the solution. The mixture was stirred for 2 h. After that, carbon black was added into the mixture and stirred overnight at room temperature. Then the suspension was filtered and washed several times with suitable amount of hot deionized water to completely remove all excess reducing agents. The remaining solid was dried in a vacuum oven for 24 h at ambient temperature. The final catalysts were 10%Pt/C, 10%Pd/C, 10%Ag/C, 10%Pd–10%Ag/C, 10%Pd–5%Ag/C, 10%Pd–15%Ag/C, 10%Pd–20%Ag/C and 10%Pd–25%Ag/C. All percentages reported here are based on weight.

2.2. Physical characterization

Structure and morphology of the catalysts were investigated using X-ray diffraction (XRD, D8 Bruker AXS X-ray diffractometer, Cu Kα radiation, 40 kV, 20 mA, 2θ range of 20–90°, scan rate 0.025°/s) and transmission electron microscopy (TEM, JEOL 3010, 200 kV). Elemental analyses were performed using energy dispersive X-ray spectroscopy (EDX, LEO 1530VP, Germany).

2.3. Electrochemical characterization

To prepare samples for electrochemical analyses, 3.3 mg of each catalyst was dispersed in 1 ml of ethanol by sonication for 2 h. Then 10 μl of this suspension was dropped onto a glassy carbon electrode (GCE, 4 mm in diameter) and dried at room temperature. 5 μl of 0.5% Nafion in ethanol was added onto GCE to fix the catalyst. Electrochemical tests were performed on an Autolab PGSTAT302 potentiostat (Eco Chemie, Netherlands) with a three-electrode cell using a Pt wire and Hg/HgO electrode (0.1 V vs. NHE) [38] as the counter and reference electrode, respectively. Blank voltammograms were done in 1 M KOH solution (blank solutions) and other tests were done in 1 M KOH + 1 M C_2H_5OH solution. N_2 was used for solution deaeration.

In order to compare the activities of different catalysts, the current obtained from electrochemical tests were normalized by using electrochemical active surface area (EASA). For 10%Pt/C, EASA value was obtained by integrating the charges in hydrogen adsorption–desorption regions by cyclic voltammetry and using a monolayer desorption charge of 210 μC/cm^2 for smooth Pt surface [39]. For Pd-based catalysts, EASA values were calculated from the PdO reduction charge, assuming a value of 405 μC/cm^2 for the reduction of PdO monolayer due to the fact that Pd on carbon exhibits a poor definition of the hydrogen region and hydrogen can penetrate into the structure of Pd-based alloys [40,41].

3. Results and discussion

3.1. Physical characterization

XRD patterns of 10%Pd/C, 10%Ag/C, 10%Pd–10%Ag/C and 10%Pt/C are shown in Fig. 1. Typical peaks of face-centered cubic (FCC) structure including (1 0 0), (2 0 0), (2 2 0) and (3 1 1) lattices are marked on all the patterns. A peak of carbon black is observed in the range of 20–30° of the diffraction spectra [42,43]. Peak position of Pd–Ag/C is between those of Pd/C and Ag/C, which suggests that an alloy of Pd and Ag was formed. Scherrer's equation was used to estimate the average size of the metal nanoparticles from (2 2 0) peaks:

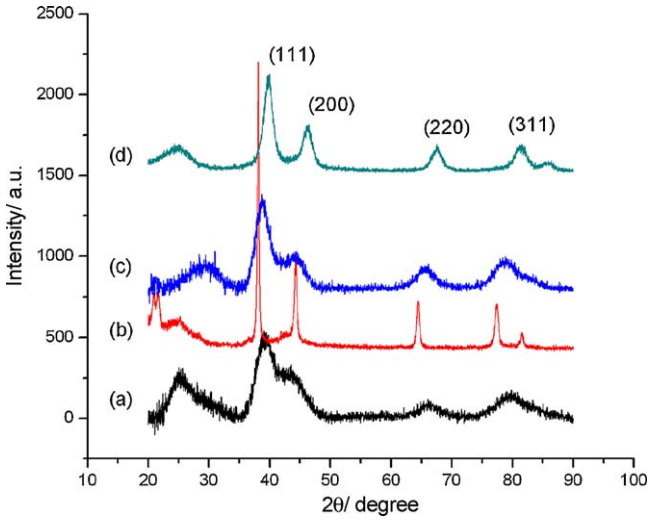

Fig. 1. XRD patterns of (a) 10%Pd/C, (b) 10%Ag/C, (c) 10%Pd–10%Ag/C and (d) 10%Pt/C.

$$d = \frac{k\lambda}{\beta\cos\theta}$$

where, k: a coefficient (0.9); λ: the wavelength of X-ray (1.54056 Å); β: the half-peak width for (2 2 0) peak (rad); θ: the angle at the (2 2 0) peak position (rad).

The average particle sizes of 10%Pt/C, 10%Pd/C, 10%Ag/C and 10%Pd–10%Ag/C are 3.8, 2.6, 15.7 and 3.7 nm, respectively (Table 1). The morphology and EDX spectra of these catalysts are shown in Fig. 2. In the case of 10%Pd–10%Ag/C, a nano-structured network was formed. The sizes of metal particles observed by TEM images are larger than those estimated by XRD data. This phenomenon was also observed by Liu et al. and Antolini et al. [44,45]. There are some possible explanations for this particle size inconsistency. The first reason is that the size calculated from XRD data is the size of single crystal particles while the TEM pictures show images of nanoparticle clusters formed from the agglomeration of single crystal particles as a result of inter-molecular forces in the synthesis process [46–48]. Another reason is that the XRD peak broadening is due not only to the crystallite size but also to the non-homogeneity of the alloy [45]. Lattice constants of 10%Pt/C, 10%Pd/C and 10%Ag/C (Table 1) calculated from d-spacing data of (2 2 0) lattices are in good agreement with the values reported (a_{Pt} = 0.392 nm; a_{Pd} = 0.389 nm; a_{Ag} = 0.409 nm) [37]. Lattice parameter value of 10%Pd–10%Ag/C which is larger than that of 10%Pd/C but smaller than that of 10%Ag/C confirmed again that a Pd–Ag alloy has been successfully formed. EDX profile of 10%Pd–10%Ag/C shows that the catalyst is composed of Pd and Ag, except for the Cu signal from the sample

Table 1
Mean particle sizes and lattice parameters of catalysts.

Catalyst	Lattice parameter, a (nm)	Average particle size, d (nm)
10%Pt/C	0.391	3.8
10%Pd/C	0.393	2.6
10%Ag/C	0.408	15.7
10%Pd–10%Ag/C	0.402	3.7

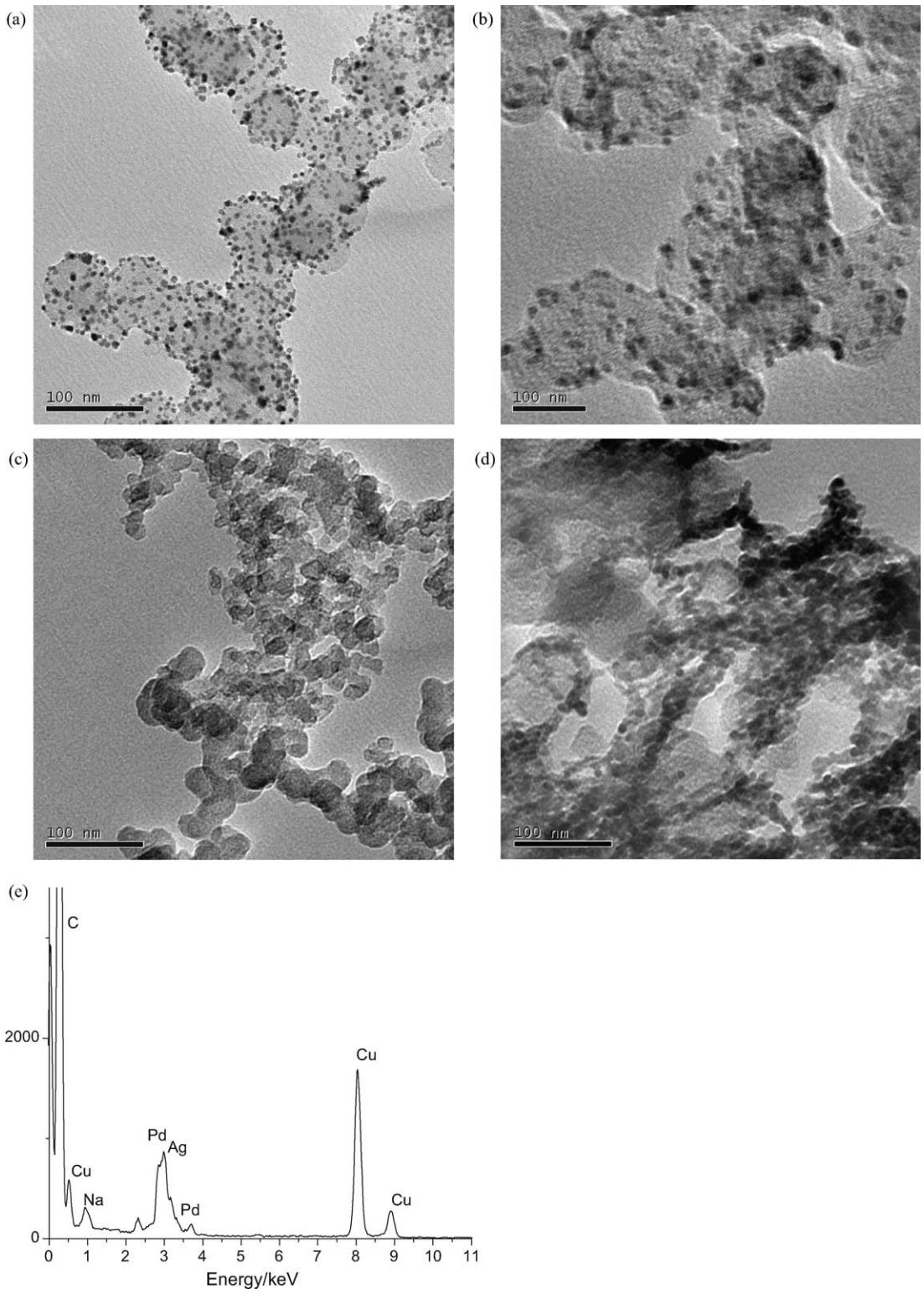

Fig. 2. TEM images of (a) 10%Pt/C, (b) 10%Pd/C, (c) 10%Ag/C, (d) 10%Pd–10%Ag/C and (e) EDX pattern of 10%Pd–10%Ag/C.

holder and some Na left from the reducing agent used for the synthesis of the catalyst.

3.2. Electrochemical tests

To investigate the activity of 10%Ag/C catalyst for ethanol oxidation in alkaline media, cyclic voltammetry (CV) tests were done in 1 M KOH solution (blank solution) and 1 M KOH + 1 M C_2H_5OH solution (Fig. 3). The CV plots of 10%Ag/C in both 1 M KOH and 1 M KOH + 1 M C_2H_5OH solutions show a pair of anodic and cathodic peaks in the range from 0.2 to 0.3 V due to the formation of silver oxide and silver oxide reduction, respectively [49–51]. There is another small reduction peak at −0.2 to −0.1 V, which belongs to the reduction of trace oxygen left in the solutions [51]. No ethanol oxidation peaks are observed for Ag/C implying that it is not active for ethanol oxidation process in alkaline media.

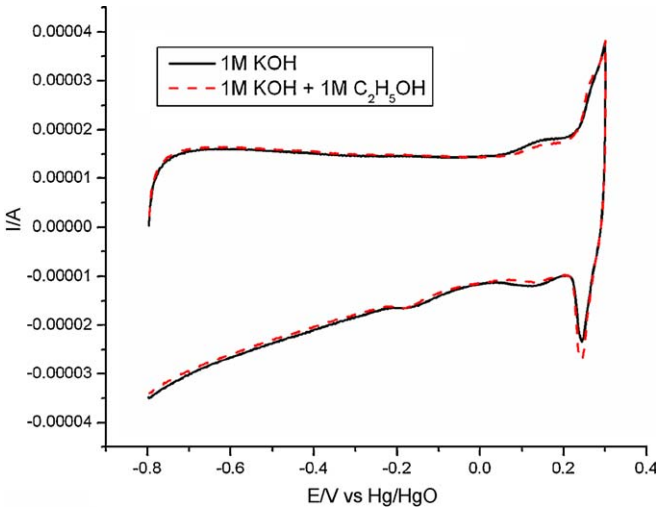

Fig. 3. CV plots of 10%Ag/C in (a) 1 M KOH and (b) 1 M KOH + 1 M C_2H_5OH with a scan rate of 50 mV/s.

The electrocatalytic activities of 10%Pt/C, 10%Pd/C and 10%Pd–10%Ag/C for ethanol oxidation reaction were characterized by linear sweep voltammetry (LSV) technique. The results normalized by electrochemical active surface area are shown in Fig. 4a. Pd/C shows a similar onset potential to that of Pt/C with a little higher peak intensity. It is evident from Fig. 4a that Ag can promote oxidation behavior of Pd/C for ethanol oxidation in alkaline environment. The oxidation onset potential on 10%Pd–10%Ag/C catalyst (ca. −0.70 V) is shifted approximately 200 mV more negative than that on 10%Pd/C (ca. −0.50 V). In addition, the peak current for 10%Pd–10%Ag/C is about 3.5 times higher than that for 10%Pd/C. This enhancement is similar to what was obtained in He et al. and Chen et al.'s works with the combinations between Pd and Au, Sn or Ru [52,53]. This fact can be explained based on the d-band center theory [29] and the mechanism recently proposed by Liang et al. [54], which will be mentioned in more details in the latter section. The lattice constant of Pd is smaller than that of Ag. Therefore, the addition of Ag to Pd causes a tensile strain in the structure of surface Pd and shifts up the d-band center of Pd [29,32]. This will improve the adsorption of OH^- onto the surface of the catalyst and thus, improve the elimination of ethoxi intermediates from the catalyst surface and help to enhance the ethanol oxidation process.

To examine the effect of Ag composition onto the ethanol oxidation activity of Pd/C, LSV tests were performed on Pd–Ag/C catalysts with different compositions of Ag (Fig. 4b). The results show that 10%Pd–10%Ag/C has the highest activity toward ethanol oxidation in terms of onset potential and peak current while 10%Pd–5%Ag/C has the lowest one. The ethanol oxidation activity of Pd–Ag/C decreases on increasing Ag composition from 10% to 25%. This is maybe due to the excessive adsorption of hydroxyl ions onto the catalyst causing a competition in adsorption between hydroxyl and ethanol species.

It is well-known that CO is a common poisoning intermediate to electrocatalysts in alcohol oxidation processes. Therefore, CO stripping tests were performed for the catalysts 10%Ag/C, 10%Pd/C, 10%Pd–5%Ag/C, 10%Pd–10%Ag/C, 10%Pd–15%Ag/C, 10%Pd–20%Ag/C and 10%Pd–25%Ag/C to compare their activities for CO oxidation. Fig. 5a displays CO tripping results for 10%Ag/C. There is no difference between CO stripping and after CO stripping curves, which indicates Ag/C has no activity for CO oxidation in alkaline media. Fig. 5b and d show that the onset potential of CO oxidation on 10%Pd–10%Ag/C (ca. −0.35 V) was more negative than that on 10%Pd/C (ca. −0.20 V). This means that the addition of Ag has facilitated the removal of CO from the surface of Pd–Ag/C. These results are in line with the higher activity of Pd–Ag/C for the

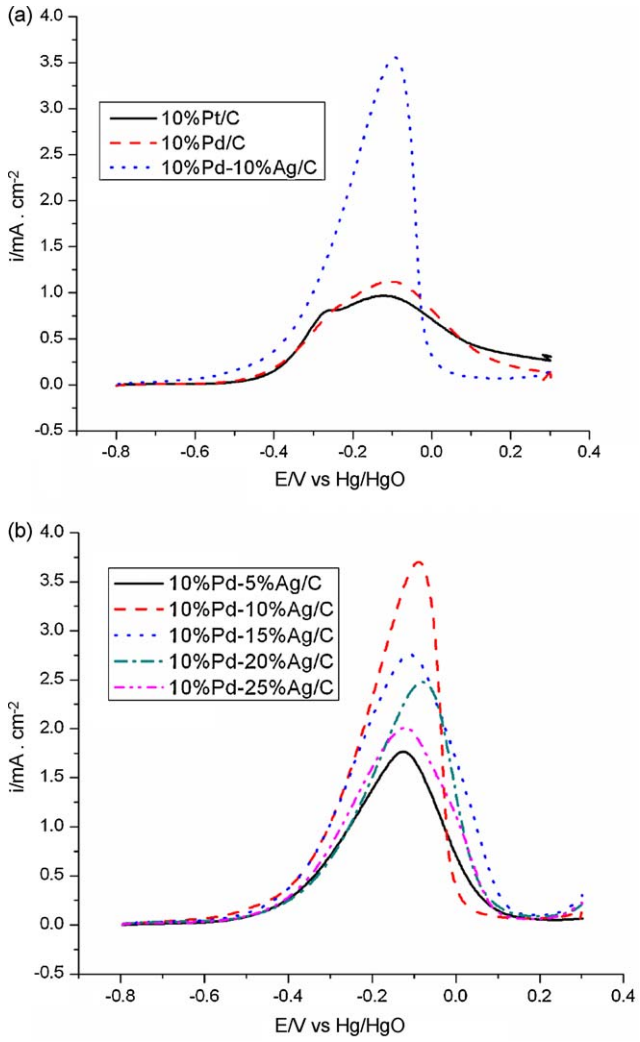

Fig. 4. Linear sweep voltammograms for ethanol oxidation on (a) 10%Pt/C, 10%Pd/C and 10%Pd–10%Ag/C and (b) 10%Pd–5%Ag/C, 10%Pd–10%Ag/C, 10%Pd–15%Ag/C, 10%Pd–20%Ag/C and 10%Pd–25%Ag/C in 1 M KOH + 1 M C_2H_5OH with 50 mV/s scan rate.

oxidation of ethanol. In addition, there exist two peaks for CO stripping on 10%Pd–10%Ag/C. Similar results are obtained for Pd–Ag/C with other ratios, as shown in Fig. 5c, e–g. The possible cause for this could be that some Pd has not been alloyed with Ag, which leads to the presence of two different types of sites for CO adsorption, i.e., Pd alone and Pd–Ag alloy. Comparing Fig. 5a and b with Fig. 5c–g, it is interesting to observe that there is no appearance of silver oxide reduction peak (ca. 0.25 V) except for palladium oxide reduction peak (ca. −0.2 V). This confirms that the upper layer of the alloy is rich of palladium.

Recently, a mechanism of the ethanol oxidation process on Pd/C in alkaline media has been proposed [54]:

$$Pd + OH^- \leftrightarrow Pd{-}OH_{ads} + e^- \quad (1)$$

$$Pd + CH_3CH_2OH \leftrightarrow Pd{-}(CH_3CH_2OH)_{ads} \quad (2)$$

$$Pd{-}(CH_3CH_2OH)_{ads} + 3OH^- \rightarrow Pd{-}(CH_3CO)_{ads} + 3H_2O + 3e^- \quad (3)$$

$$Pd{-}(CH_3CO)_{ads} + Pd{-}OH_{ads} \rightarrow Pd{-}CH_3COOH + Pd : \text{slow} \quad (4)$$

$$Pd{-}CH_3COOH + OH^- \rightarrow Pd + CH_3COO^- + H_2O : \text{fast} \quad (5)$$

The rate-determining step is proposed to be step (4), in which the adsorbed ethoxi intermediate is removed by adsorbed

hydroxyl ions to form acetate as the main product and release free active catalytic sites. As shown in Fig. 5, CVs of Pd/C and Pd–Ag/C catalysts in N_2-saturated solutions (dashed lines) show a peak around −0.25 V in forward scan, which is assigned to OH^- adsorption [54,55]. The OH^- adsorption peak potentials are −0.247 V, −0.261 V, −0.272 V, −0.279 V, −0.287 V and −0.291 V for 10%Pd/C, 10%Pd–5%Ag/C, 10%Pd–10%Ag/C, 10%Pd–15%Ag/C, 10%Pd–20%Ag/C and 10%Pd–25%Ag/C, respectively. This phenomenon indicates that OH^- ions are more easily adsorbed onto Pd–Ag/C than Pd/C. According to reaction (4), this helps to remove more intermediates and release more active sites on the surface of the catalyst. The tendency becomes more apparent with the increase of Ag component in the catalyst and can also be explained by d-band center theory. When more Ag is added into the structure of Pd, more upshift of d-band center is achieved. As a result, more OH^- is adsorbed onto the catalyst surface and thus, more active sites are released via reaction (4). However, excess adsorption of OH^- also causes a competition with the adsorption of ethanol. This could be

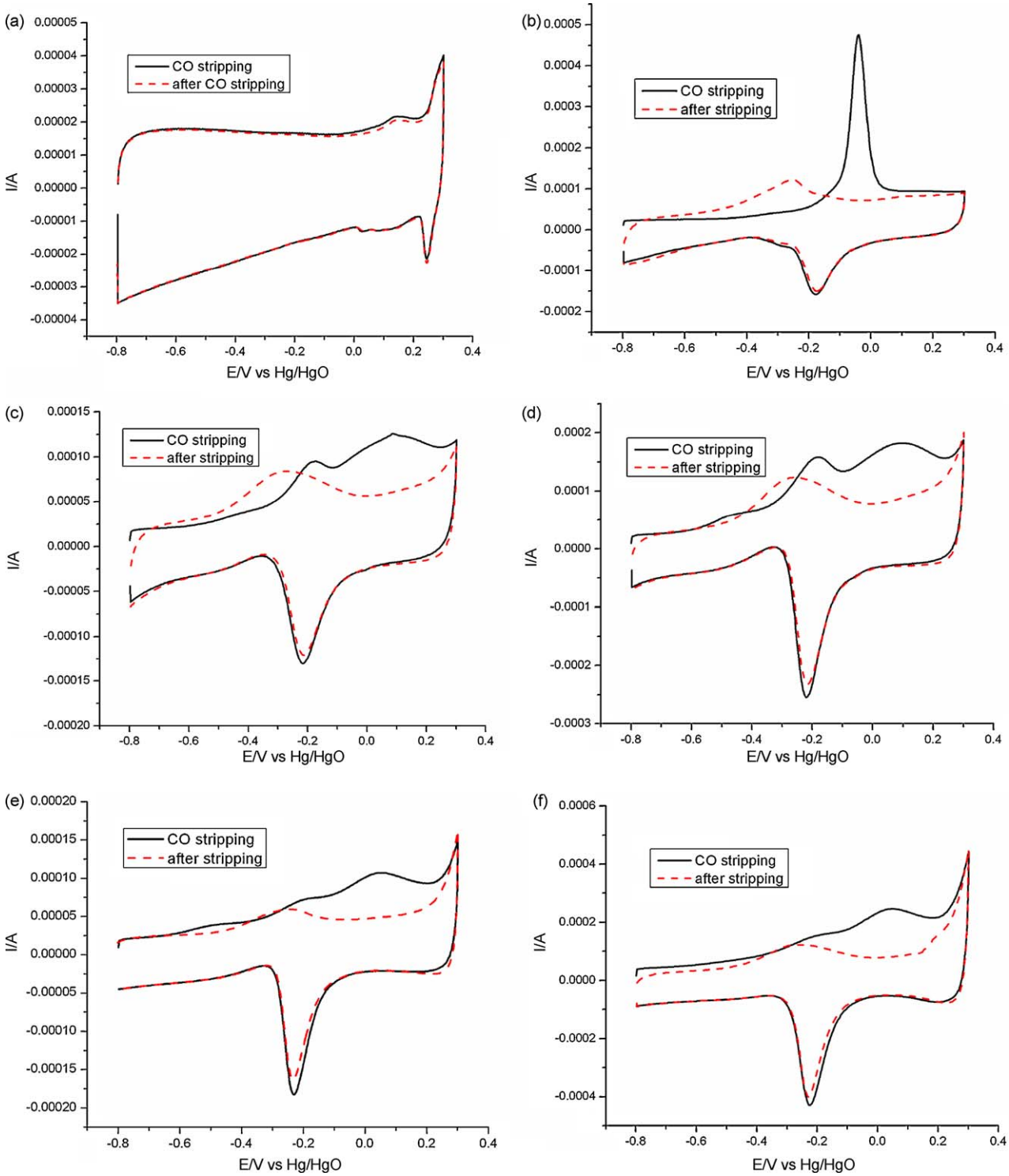

Fig. 5. CO stripping voltammograms for (a) 10%Ag/C, (b) 10%Pd/C, (c) 10%Pd–5%Ag/C, (d) 10%Pd–10%Ag/C, (e) 10%Pd–15%Ag/C, (f) 10%Pd–20%Ag/C and (g) 10%Pd–25%Ag/C in 1 M KOH solution; scan rate: 50 mV/s.

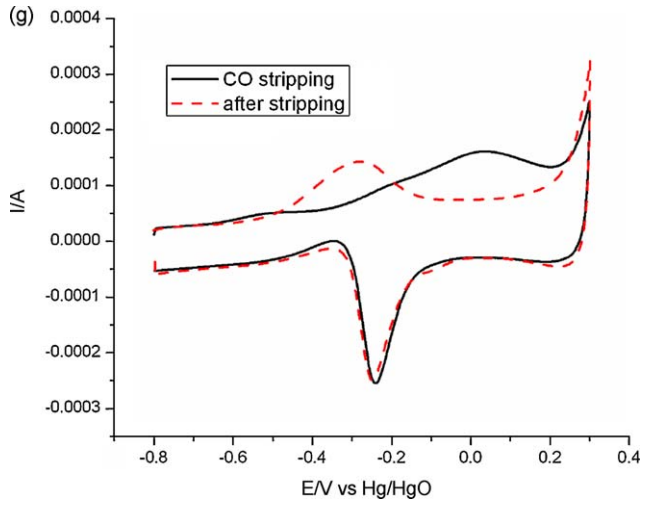

Fig. 5. (*Continued*).

the possible reason for the activity decrease on the catalysts when the Ag composition increases from 10% to 25%. Ag was reported to adsorb OH^- at rather low potentials (−0.9 to −0.4 V vs. Hg/HgO) [49,56,57] and this feature may also contribute to the more negative values of the OH^- adsorption potential of Pd–Ag/C catalysts. However, the surface layer of the alloy is rich of Pd and therefore, the affinity of Ag for OH^- just plays a small role in the ethanol oxidation improvement.

To evaluate both the steady-state activity towards ethanol oxidation and the poisoning of the catalysts, chronoamperometric (CA) measurements were carried out at −0.25 V for 1000 s in the solution of 1 M KOH + 1 M C_2H_5OH. In all the three CA curves displayed in Fig. 6a, the current drops sharply during the first few minutes and then becomes relatively stable. Firstly, the active sites are free from adsorbed ethanol; after that, the adsorption of new ethanol molecules would depend on the liberation of the active sites by the oxidation of ethanol or intermediates, such as ethoxi or CO-like species, formed during the first few minutes, which poisons the active surface. It can be seen that at the beginning, the current for 10%Pt/C is the highest but then decreases much faster than that for other catalysts and becomes the lowest one. This phenomenon is due to the fact that Pt is more easily poisoned by CO-containing intermediates [13,15,58]. In the stable stage, the current produced by 10%Pd–10%Ag/C is the highest, indicating the better CO tolerance feature of this catalyst. Fig. 6b shows CA curves for Pd–Ad/C catalysts with different compositions of Ag. The results indicate that 10%Pd–10%Ag/C is the best poisoning-tolerant catalyst and 10%Pd–5%Ag/C is the worst one, among all the catalysts investigated. Current values of Pd–Ag/C catalysts decrease when Ag content further increases from 10% to 25%. This trend, consistent with the LSV result, may be explained by the

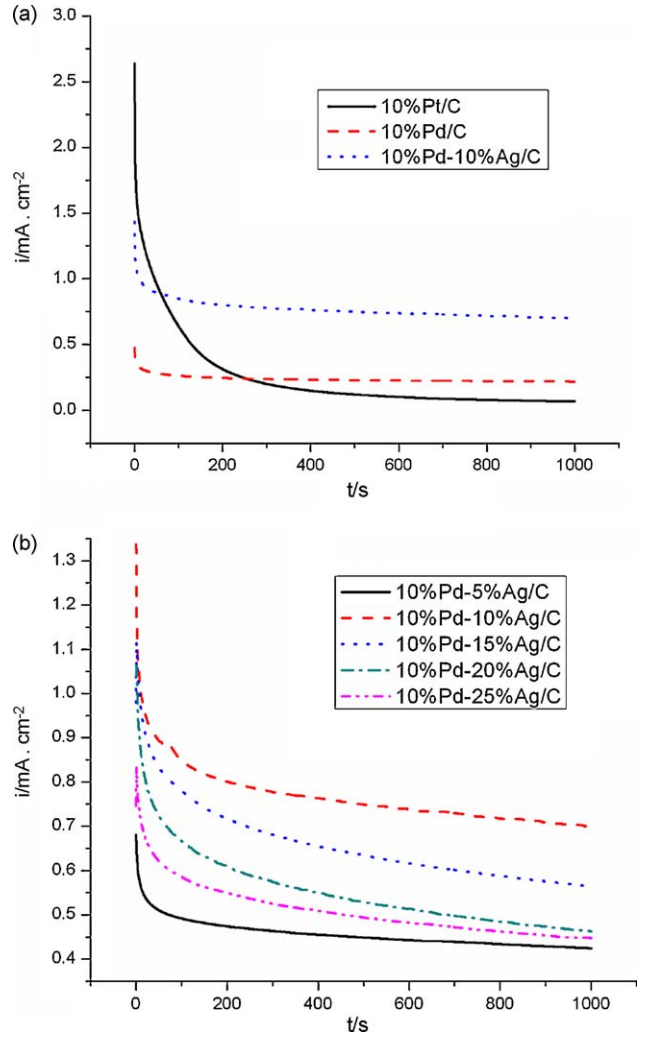

Fig. 6. Chonoamperometric curves for (a) 10%Pt/C, 10%Pd/C and 10%Pd–10%Ag/C and (b) 10%Pd–5%Ag/C, 10%Pd–10%Ag/C, 10%Pd–15%Ag/C, 10%Pd–20%Ag/C and 10%Pd–25%Ag/C in 1 M KOH + 1 M C_2H_5OH solution at −0.25 V (vs. Hg/HgO).

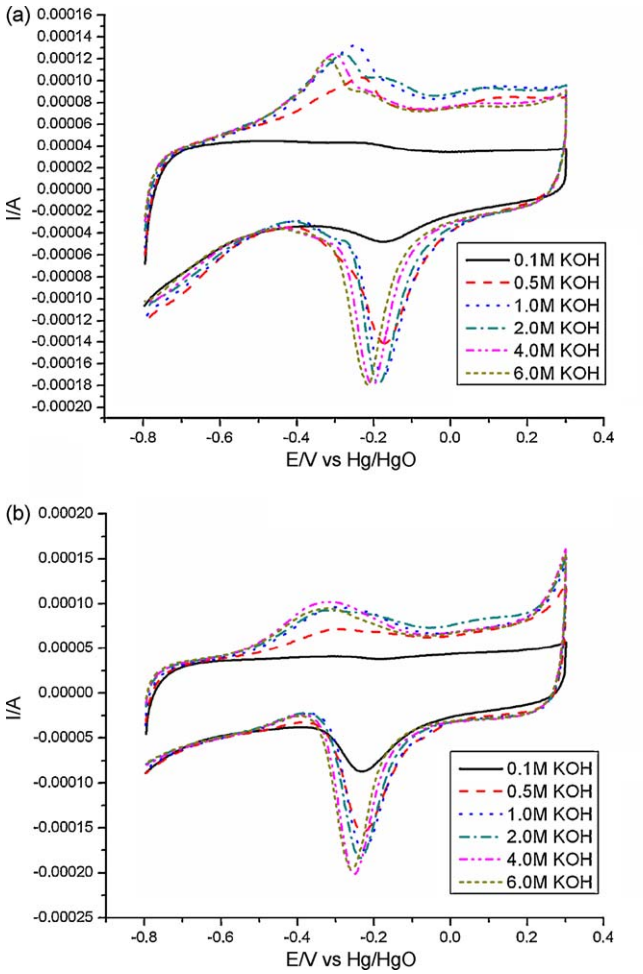

Fig. 7. Blank CVs of (a) Pd/C and (b) Pd–Ag/C in different KOH solutions; scan rate: 50 mV/s.

same argument, i.e., the adsorption competition between ethanol and hydroxyl group with excess Ag. In consequence, less poisoning species are removed to free active sites and the catalysts become less stable.

For better understanding the adsorption of hydroxyl ions onto Pd/C and Pd–Ag/C catalysts, blank CV tests were performed for Pd/C and Pd–Ag/C in solutions with different concentrations of KOH (Fig. 7). At low OH^- concentration (0.1 M), no clear peaks for hydroxyl adsorption can be observed for both of the catalysts. When the OH^- concentration is increased from 0.5 to 6 M, clear hydroxyl adsorption peaks appear. Fig. 7 and Table 2 display the adsorption peak potential values for the two catalysts. The results show a negative shift in hydroxyl adsorption peak potentials on both of the catalysts when the OH^- concentration goes up. The possible reason for this trend is the adsorption of hydroxyl ion onto the active sites of the catalysts is more favorable when there are more hydroxyl ions in the solution. Another observation is that the OH^- adsorption peak potential for Pd–Ag/C is always more

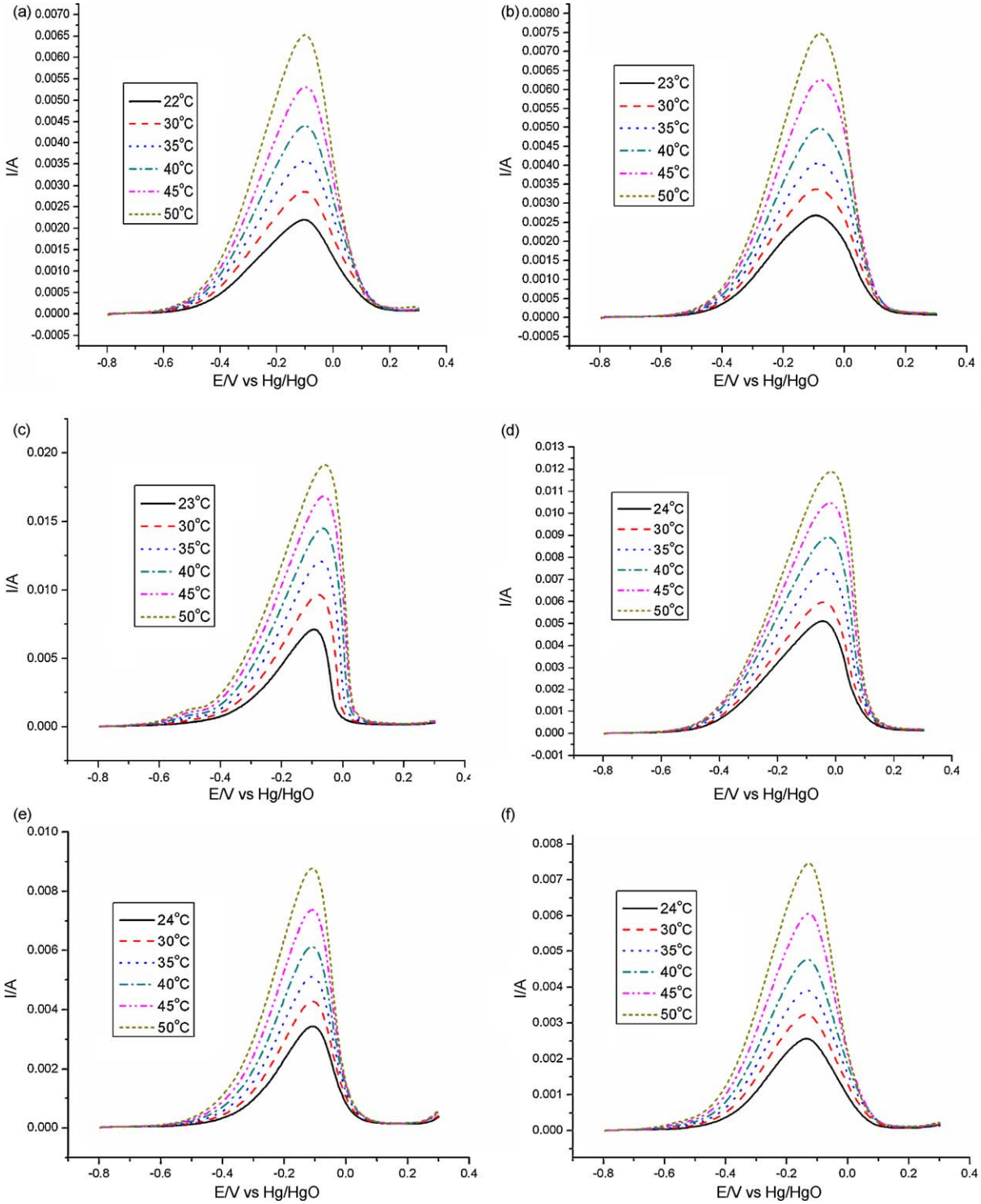

Fig. 8. LSV tests in 1 M KOH + 1 M C_2H_5OH solutions at different temperatures for (a) 10%Pd/C, (b) 10%Pd–5%Ag/C, (c) 10%Pd–10%Ag/C, (d) 10%Pd–15%Ag/C, (e) 10%Pd–20%Ag/C and (f) 10%Pd–25%Ag/C; scan rate: 50 mV/s.

Table 2
OH^- adsorption peak potential values for Pd/C and Pd–Ag/C in blank solutions with different concentrations of KOH.

KOH concentration (M)	0.1	0.5	1.0	2.0	4.0	6.0
OH adsorption peak potential (V) for Pd/C	No peak	−0.235	−0.249	−0.278	−0.301	−0.318
OH adsorption peak potential (V) for Pd–Ag/C	No peak	−0.292	−0.301	−0.317	−0.317	−0.324

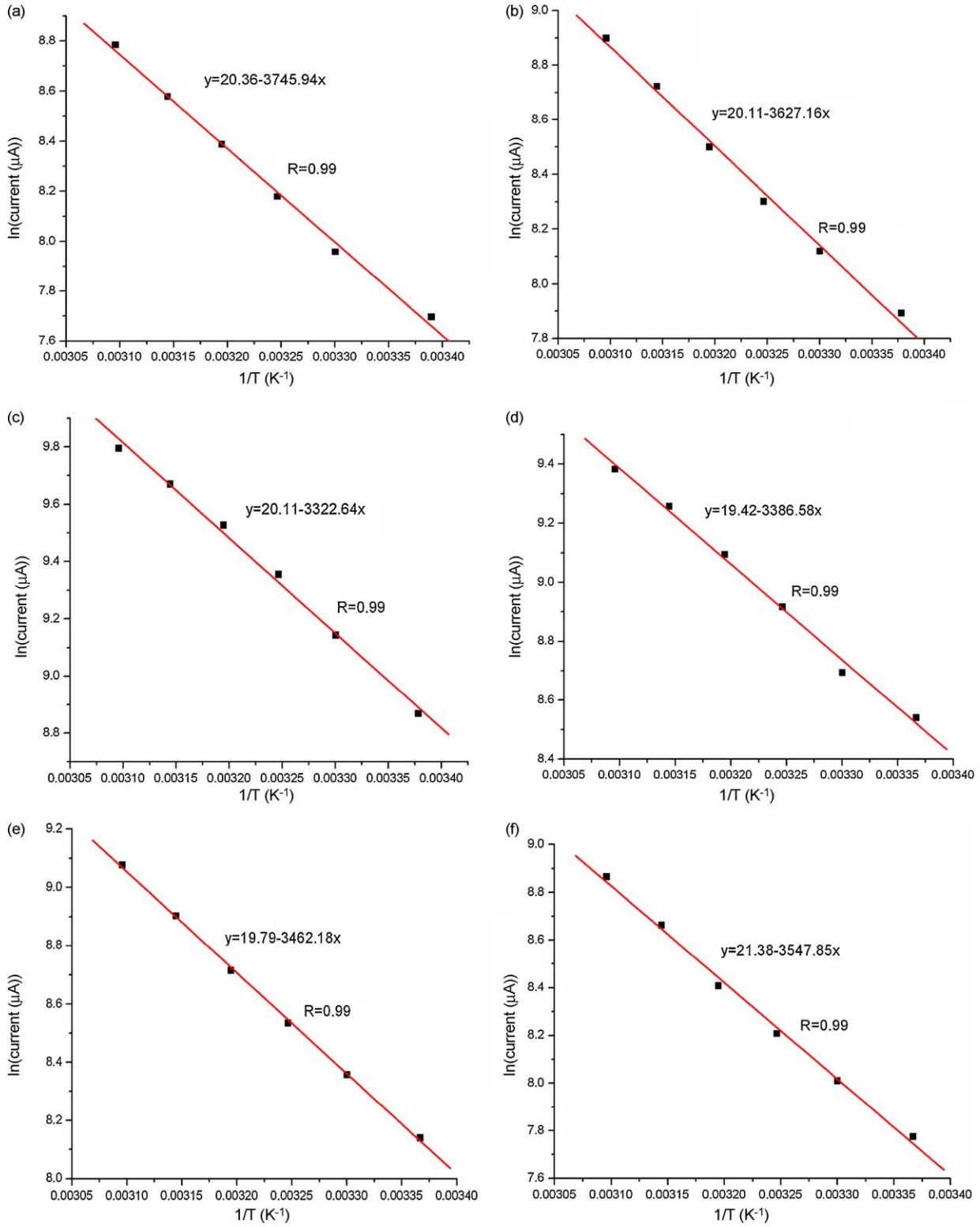

Fig. 9. Arrhenius plots for (a) 10%Pd/C, (b) 10%Pd–5%Ag/C, (c) 10%Pd–10%Ag/C, (d) 10%Pd–15%Ag/C, (e) 10%Pd–20%Ag/C and (f) 10%Pd–25%Ag/C at −0.1 V.

negative than that for Pd/C at the same OH^- concentration value. This fact again confirms the alloyed catalyst facilitates the adsorption of OH^-.

Beside the promotion effect of Ag, another possible reason for the high activity of Pd–Ag/C is the special morphology of this catalyst. The TEM picture in Fig. 2d shows a network structure of Pd–Ag/C. It means the Pd–Ag nanoparticles are interconnected. The interconnected network possesses more boundary defects (such as steps and kinks) than individual particles. Therefore, it has more active catalytic sites for OH^- adsorption and ethanol oxidation [59].

To exclude the effect of other factors, such as the catalyst surface area, on the resulting current, LSV tests in 1 M KOH + 1 M C_2H_5OH solution was performed at different temperatures for 10%Pd/C, 10%Pd–5%Ag/C, 10%Pd–10%Ag/C, 10%Pd–15%Ag/C, 10%Pd–20%Ag/C and 10%Pd–25%Ag/C (Fig. 8). From the abstracted data, Fig. 9 is plotted and the activation energy values were calculated based on Arrhenius equation [60] as below:

$$\ln I = \frac{\ln A - E_a}{(RT)}$$

where, I: current at a specific potential; R: gas constant, 8.314 J/(mol K); T: temperature in K; E_a: activation energy at a specific potential.

At the same potential of 0.1 V, the lowest value of 27.6 kJ/mol for the ethanol oxidation on 10%Pd–10%Ag/C is obtained as against the highest value of 31.1 kJ/mol on 10%Pd/C. The activation energy values for 10%Pd–5%Ag/C, 10%Pd–15%Ag/C, 10%Pd–20%Ag/C and 10%Pd–25%Ag/C are 30.2, 28.2, 28.8 and 29.5 kJ/mol, respectively. The lower E_a means a higher intrinsic activity for the Pd–Ag/C, as the effect of catalyst surface area has been excluded. This result is consistent with the above observations.

4. Conclusions

In this study, the high activity of Pd–Ag/C catalysts towards ethanol oxidation in alkaline media in comparison with Ag/C, Pt/C and Pd/C was reported. The catalyst was synthesized with $NaBH_4$ as a reducing agent and sodium citrate as a stabilizer. XRD results showed the formation of alloy structure for the Pd–Ag/C. Electrochemical measurements indicated that it possessed a better intrinsic activity towards ethanol oxidation than Pt/C and Pd/C and the best performance was observed for 10%Pd–10%Ag/C. This makes Pd–Ag/C a promising anodic catalyst for alkaline DEFC.

Acknowledgments

The authors gratefully acknowledge Academic research fund AcRF tier 1 (RG40/05), AcRF tier 2 (ARC11/06) from the Ministry of Education, Singapore and a graduate scholarship from AUN/SEEDNet-JICA.

References

[1] L. Zhang, J. Zhang, D.P. Wilkinson, H. Wang, Journal of Power Sources 156 (2006) 171–182.
[2] H.B. Suffredini, G.R. Salazar-Banda, L.A. Avaca, Journal of Power Sources 171 (2007) 355–362.
[3] F. Vigier, S. Rousseau, C. Coutanceau, J.M. Leger, C. Lamy, Topics in Catalysis 40 (2006) 111–121.
[4] S. Song, Y. Wang, P. Shen, Chinese Journal of Catalysis 28 (2007) 752–754.
[5] S. Song, P. Tsiakaras, Applied Catalysis B: Environmental 63 (2006) 187–193.
[6] K. Taneda, Y. Yamazaki, Electrochimica Acta 52 (2006) 1627–1631.
[7] S. Wang, S.P. Jiang, X. Wang, Nanotechnology 19 (2008) 265601.
[8] S. Wang, X. Wang, S.P. Jiang, Langmuir 24 (2008) 10505–10512.
[9] X. Wang, M. Waje, Y. Yan, Journal of the Electrochemical Society 151 (2004) 2183–2188.
[10] E. Antolini, Journal of Power Sources 170 (2007) 1–12.
[11] F. Hu, C. Chen, Z. Wang, G. Wei, P.K. Shen, Electrochimica Acta 52 (2006) 1087–1091.
[12] C. Lamy, S. Rousseau, E.M. Belgsir, C. Coutanceau, J.M. Leger, Electrochimica Acta 49 (2004) 3901–3908.
[13] H. Li, G. Sun, L. Cao, L. Jiang, Q. Xin, Electrochimica Acta 52 (2007) 6622–6629.
[14] F. Delime, J.M. Leger, C. Lamy, Journal of Applied Electrochemistry 28 (1997) 27–35.
[15] J. Ribeiro, D.M. Dos Anjos, J.M. Leger, F. Hahn, P. Olivi, A.R. De Andrade, G. Tremiliosi-Filho, K.B. Kokoh, Journal of Applied Electrochemistry 38 (2008) 653–662.
[16] N. Wagner, M. Schulze, E. Gulzow, Journal of Power Sources 127 (2004) 264–272.
[17] C. Xu, L. Cheng, P. Shen, Y. Liu, Electrochemistry Communications 9 (2007) 997–1001.
[18] H. Liu, W. Li, A. Manthiram, Applied Catalysis B: Environmental 90 (2009) 184–194.
[19] A. Serov, C. Kwak, Applied Catalysis B: Environmental 90 (2009) 313–320.
[20] H.T. Zheng, Y. Li, S. Chen, P.K. Shen, Journal of Power Sources 163 (2006) 371–375.
[21] P.K. Shen, C. Xu, Electrochemistry Communications 8 (2006) 184–188.
[22] C. Xu, P.k. Shen, Y. Liu, Journal of Power Sources 164 (2007) 527–531.
[23] J. Ye, J. Liu, C. Xu, S.P. Jiang, Y. Tong, Electrochemistry Communications 9 (2007) 2760–2763.
[24] F.P. Hu, P.K. Shen, Journal of Power Sources 173 (2007) 877–881.
[25] C. Xu, Z. Tian, P. Shen, S.P. Jiang, Electrochimica Acta 53 (2008) 2610–2618.
[26] L.D. Zhu, T.S. Zhao, J.B. Xu, Z.X. Liang, Journal of Power Sources 187 (2009) 80–84.
[27] R.N. Singh, A. Singh, Anindita, Carbon 47 (2009) 271–278.
[28] U.B. Demirci, Journal of Power Sources 173 (2007) 11–18.
[29] B. Hammer, J.K. Nørskov, Theoretical surface science and catalysis-calculations and concepts, Advances in Catalysis (2000) 71–129.
[30] J. Zhang, M.B. Vukmirovic, Y. Xu, M. Mavrikakis, R.R. Adzic, Angewandte Chemie – International Edition 44 (2005) 2132–2135.
[31] J. Greeley, J.K. Nørskov, Surface Science 592 (2005) 104–111.
[32] J. Greeley, J.K. Nørskov, M. Mavrikakis, Electronic structure and catalysis on metal surfaces, Annual Review of Physical Chemistry (2002) 319–348.
[33] V. Stamenkovic, B.S. Mun, K.J.J. Mayrhofer, P.N. Ross, N.M. Markovic, J. Rossmeisl, J. Greeley, J.K. Nørskov, Angewandte Chemie – International Edition 45 (2006) 2897–2901.
[34] B. Hammer, J.K. Norskov, Surface Science 343 (1995) 211–220.
[35] F.H.B. Lima, J. Zhang, M.H. Shao, K. Sasaki, M.B. Vukmirovic, E.A. Ticianelli, R.R. Adzic, Journal of Physical Chemistry C 111 (2007) 404–410.
[36] A. Ruban, B. Hammer, P. Stoltze, H.L. Skriver, J.K. Nørskov, Journal of Molecular Catalysis A: Chemical 115 (1997) 421–429.
[37] W.F. Smith, Principles of Materials Science and Engineering, 3rd ed., McGraw-Hill, Inc., New York, 1996.
[38] E.E. Switzer, T.S. Olson, A.K. Datye, P. Atanassov, M.R. Hibbs, C.J. Cornelius, Electrochimica Acta 54 (2009) 989–995.
[39] A. Pozio, M. De Francesco, A. Cemmi, F. Cardellini, L. Giorgi, Journal of Power Sources 105 (2002) 13–19.
[40] R. Pattabiraman, Applied Catalysis A: General 153 (1997) 9–20.
[41] M. Lukaszewski, M. Grden, A. Czerwinski, Journal of Solid State Electrochemistry 9 (2005) 1–9.
[42] W.J. Zhou, W.Z. Li, S.Q. Song, Z.H. Zhou, L.H. Jiang, G.Q. Sun, Q. Xin, K. Poulianitis, S. Kontou, P. Tsiakaras, Journal of Power Sources 131 (2004) 217–223.
[43] T. Lopes, E. Antolini, F. Colmati, E.R. Gonzalez, Journal of Power Sources 164 (2007) 111–114.
[44] Z. Liu, X.Y. Ling, X. Su, J.Y. Lee, Journal of Physical Chemistry B 108 (2004) 8234–8240.
[45] E. Antolini, F. Colmati, E.R. Gonzalez, Electrochemistry Communications 9 (2007) 398–404.
[46] G. Cao, Nanostructures & Nanomaterials: Synthesis, Properties & Applications, Imperial College Press, London, 2004.
[47] A. Muramatsu, in: Y. Waseda, A. Muramatsu (Eds.), Morphology Control of Materials and Nanoparticles, Springer, Berlin, 2004, p. 30.
[48] H. Abe, F. Matsumoto, L.R. Alden, S.C. Warren, H.D. Abruna, F.J. DiSalvo, Journal of the American Chemical Society 130 (2008) 5452–5458.
[49] B.B. Blizanac, P.N. Ross, N.M. Markovic, Journal of Physical Chemistry B 110 (2006) 4735–4741.
[50] S.L. Horswell, A.L.N. Pinheiro, E.R. Savinova, M. Danckwerts, B. Pettinger, M.-S. Zei, G. Ertl, Langmuir 20 (2004) 10970–10981.
[51] F.H.B. Lima, J.F.R. de Castro, E.A. Ticianelli, Journal of Power Sources 161 (2006) 806–812.
[52] Q. He, W. Chen, S. Mukherjee, S. Chen, F. Laufek, Journal of Power Sources 187 (2009) 298–304.
[53] Y. Chen, L. Zhuang, J. Lu, Chinese Journal of Catalysis 28 (2007) 870–874.
[54] Z.X. Liang, T.S. Zhao, J.B. Xu, L.D. Zhu, Electrochimica Acta 54 (2009) 2203–2208.
[55] J. Prabhuram, R. Manoharan, H.N. Vasan, Journal of Applied Electrochemistry 28 (1998) 935–941.
[56] B.B. Blizanac, P.N. Ross, N.M. Markovic, Electrochimica Acta 52 (2007) 2264–2271.
[57] I. Boskovic, S.V. Mentus, M. Pjescic, Electrochimica Acta 51 (2006) 2793–2799.
[58] A.V. Tripkovic, K.D. Popovic, J.D. Lovic, Electrochimica Acta 46 (2001) 3163–3173.
[59] A.N. Gavrilov, E.R. Savinova, P.A. Simonov, V.I. Zaikovskii, S.V. Cherepanova, G.A. Tsirlina, V.N. Parmon, Physical Chemistry Chemical Physics 9 (2007) 5476–5489.
[60] J.L. Cohen, D.J. Volpe, H.D. Abruna, Physical Chemistry Chemical Physics 9 (2007) 49–77.